Face Selective Neural Activity: comparison between fixed and free viewing

Carmel R. Auerbach-Asch (1), Oded Bein (2), Prof. Leon Y. Deouell (1,2)

1. The Edmond and Lily Safra Center for Brain Sciences, The Hebrew University of Jerusalem, Edmond J. Safra Campus, Givat-Ram, Jerusalem 91904, Israel
2. The Department of Psychology, The Hebrew University of Jerusalem, Mount Scopus, Jerusalem 91905, Israel

Corresponding Author:

1. Name: Carmel Ruth Auerbach-Asch,
2. Email: carmel.auerbach@gmail.com
3. Tel: +972-549702220
4. ORCHID No.: 0000-0001-6996-1350

Key words: Fixation Related Potentials (FRP), N170, Faces, EEG, Eye tracking, Free-Viewing

Acknowledgements – This work is supported by grant 1902/14 from the Israel Science Foundation to L.Y.D. We thank Dr. Edden Gerber for his matlab implementation of the pre-processing procedure. We thank all research assistants who helped with data collection and Namoi Revel, who helped with formatting the bibliography.

Abstract

Event Related paradigms (ERPs) are widely used to study category-selective EEG responses to visual stimuli, such as the face-selective N170 component. While allowing for good experimental control these paradigms ignore the dynamic role of eye-movements in natural vision. Fixation-related potentials (FRPs) obtained using simultaneous EEG and eye-tracking overcome this limitation. While various studies have used FRPs to study processes such as lexical processing, target detection and attention allocation, no study has directly examined categorical visual recognition in free-viewing conditions. The goal of this study was to compare the well-known face-sensitive activity evoked by stimulus abrupt appearance (N170 component) with that evoked by self-controlled fixations on a stimulus. Twelve subjects were studied in three experimental conditions: Free-viewing (FRPs), Cued-viewing(FRPs) and Control (ERPs). We used a multiple regression GLM approach to disentangle overlapping components. Our results show that the N170 face differential effect (face vs. non-face) is evident for the first fixation on a stimulus, whether it follows a self-generated saccade or stimulus appearance at fixation point. Whereas the N170 differential effect has similar topography across viewing conditions, there are major differences between ERP and FRP activity within each stimulus category. We hypothesized that the fixation-related Lambda complex may overlap the N170 in FRPs, and establish the plausibility of this account using hypothesis-driven dipole simulations. This study establishes the use of the N170 effect as a signature of face detection in free viewing experiments while highlighting the importance of accounting for fixation-specific effects.

Introduction

The processing of faces has been a prominent object of interest in both eye-movement research examining gaze allocation on faces (Henderson et al., 2005; Hsiao et al., 2008; Yarbus, 1967; Min et al., 2015) and in EEG research examining brain activity unique to face processing (Bentin et al., 1996; Rossion et al., 2000a; Rousselet et al., 2004). The latter experiments were conducted using event-related paradigms (ERPs), and more recently in frequency-tagging paradigms (Rossion, 2014), in both of which eye movements are restricted and stimuli are abruptly flashed at fixation point. Such paradigms reduce signal artifacts caused by the eye movements, but ignore the dynamics of natural vision and the possible role that active sampling has on perception (Martinez-Conde et al., 2004; Schroeder et al., 2010). They also limit the type of experiments which can be done. Co-registration of eye-movements and electroencephalography (EEG) provides a powerful tool for studying visual perception in a more natural setting (Dimigen et al., 2011; Nikolaev et al., 2016). Such studies examine the EEG activity locked to either fixation- or saccade-onset (Fixation- or saccade-related potentials; FRPs, SRPs) rather than to an abrupt stimulus onset. s

Using SRPs or FRPs, recent studies examined neural responses in reading (Baccino & Manunta, 2005; Dimigen et al., 2011; Frey et al., 2013) visual search (Devillez et al., 2015; Kaunitz et al., 2014), free picture viewing (Fischer et al., 2013; Nikolaev et al., 2013), target detection (Brouwer et al., 2013; Kamienkowski et al., 2012), and spatial attention (Meyberg et al., 2017). Some of these studies have directly compared well known ERP components evoked by a stimulus onset to those evoked by fixation onsets, such as the P1 (Kazai & Yagi, 2003), the N400 (Dimigen et al., 2011; Hutzler et al., 2007) and the P3 (Kamienkowski et al., 2012). Other FRP studies have used face images to test effects such as target detection or effects of prediction (Dimigen et al., 2009; Ehinger & Dimigen, 2018; Huber-Huber et al., 2019; Kaunitz et al., 2014), yet did not compare face-selective activity, that is, the difference between the response to faces and other stimuli, between ERPs and FRPs. The careful examination of categorical processing comparing free viewing and static gaze conditions is important for future interpretation of categorical processing and object identification in free-viewing studies.

Studies using ERPs consistently find that faces induce a larger negativity when compared to non-face stimuli, peaking at ~170ms after stimulus onset with a maximum at occipito-temporal electrode sites

(N170 effect - Bentin et al., 1996; Rossion et al., 2000b) In a free viewing scenario, the early latency of this response would be especially prone to interaction with both overlap of responses from previous fixations or eye movements, as well as with robust fixation-specific visual responses.

Here, we set out to test the face-selective N170 effect in free-viewing. Specifically, we compared face-selective activity (face vs. non-face) following a saccade to stimuli at the periphery, to face-selective activity evoked by an abrupt appearance of the stimuli at a fixation point. In both paradigms neural activity is locked to the first instance in which categorical information of the object is available[1]. However, there are differences between the two scenarios in the temporal predictability of the input, the amount of retinal changes and the type of motor activity. For example, the lambda wave, a sharp positive component with a peak latency of about 80 ms from the offset of saccade (Yagi, 1979) is a prominent component of FRPs believed to be elicited by the major change of input across the retina (Volkmann, 1986).

An additional methodological challenge of FRP research is the overlapping activity due to the temporal proximity of experimentally-uncontrolled sequential fixations (Dimigen et al., 2011; Nikolaev et al., 2016). Since fixation durations are not uniformly distributed, FRP distortions may be systematic and thus may appear even after trial averaging. Some recent studies addressed this issue by including a procedure of matching eye movement characteristics such as size, direction, and duration, across experimental conditions, in order to balance out distortions (Devillez et al., 2015; Fischer et al., 2013; Kamienkowski et al., 2012; Nikolaev et al., 2016). Other studies included a training period to encourage long fixations (Kamienkowski et al., 2012; Kaunitz et al., 2014). Here, we avoided the need for fixation selection (entailing data loss and biased sampling) or participant training (entailing unnatural conditions) by adopting a multiple regression framework for de-convolving overlapping responses using the continuous data from all trials (Dandekar et al., 2012a; Ehinger & Dimigen, 2018; Smith & Kutas, 2015b), similarly to techniques used in fMRI analysis.

[1] In our design, object identification of the peripheral stimulus was not possible before the saccade.

Materials and Methods

Participants

13 healthy adults with normal eye-vision and no reported neurological illness participated in the experiment (7 females and 6 males; age range 19-29 years, Mean=23.3 years). One participant was omitted from analysis due to excessive signal artifacts. All participants were students of the Hebrew University of Jerusalem, received payment or class credit for their participation. Informed consent was obtained from all individual participants included in the study. The study was approved by the ethics committee of the Hebrew University of Jerusalem and conducted according to the principles expressed in the 1964 Declaration of Helsinki.

Stimuli and Experimental Apparatus

Stimuli consisted of 170 pictures of faces and 170 pictures of painted eggs, all gray-scale with equated luminance and contrast (same as used in Amihai et al., 2011). Faces were stripped of hair and presented in an oval aperture. Painted eggs were chosen because of their general resemblance to faces, being oval and with internal detail. All pictures were imposed on a square gray-scale clouds-like background, which hindered identification of the objects before fixating on them (see example in figure 1). The fixation symbol at the center of the screen consisted of a light gray dot surrounded by 4 light gray arrows. Participants were seated 100cm from the screen (Viewsonic G75f Cathode Ray Tube), and the overall size of the stimuli was ~1.84° x 1.84 visual angles. The stimuli appeared on a gray background, with screen resolution set to 1024 X 768, and a 100Hz refresh-rate.

Experimental Procedure

The experiment included three conditions: Cued-Viewing, Uncued-Viewing, and Control (Figure 1). All three conditions had a similar structure, but crucially, they differed in how constrained were the participants' eye movements.

In the *Cued-Viewing* condition, a trial started with the appearance of the fixation symbol. Once the participant maintained fixation for 100 ms (monitored by the eye-tracker), two stimuli appeared in the upper corners of the screen while participants were instructed to maintain center fixation. 300-700 ms after the stimulus onset, the participants received a cue informing them of the target stimulus to which they should perform an immediate saccade. The cue was the simultaneous highlighting of one of the central arrows, and a peripheral white dot in the center of the target stimulus, serving together as a combination of endogenous and exogenous cues. Stimuli remained on the screen for an additional 700-

1100ms, constraining the viewing time in each trial and promoting quick eye movement reaction to the cue. Finally, a question mark appeared at the screen center and participants were required to move their gaze centrally and indicate with a button press whether the cued stimulus was a face or not.

In the *Uncued-Viewing* condition, a trial started again with the appearance of the fixation symbol. Once the participant maintained fixation for 100 ms, 4 stimuli consisting of a random combination of eggs and faces appeared at the corners of the screen. 300-700 ms later the center fixation symbol disappeared cuing the participants to freely examine the 4 corner stimuli at their own pace and in any desired order. The behavioral task was to report the number of faces (out of the 4 stimuli) in each trial.

[Figure 1 about here]

Fig. 1 Experimental design of each block: a. The Cued-viewing condition started with a fixation on the screen center followed by stimulus appearance (S) in periphery while center fixation is maintained (screens 1-2; the numbers are for the sake of illustration and were not presented to subjects). After 300-700 ms an arrow cue (C) indicated the stimulus on which the participants should fixate (F1 - screen 4). After preforming a saccade to the cued stimulus, participants returned their gaze to the center and reported (R) if the cued stimulus was an egg or a face (screen 5). b. The Uncued-viewing condition started like the cued-viewing condition (screens 1-2, notice there were 4 stimuli in this condition as opposed to 2 in the Cued block). Screen 3 depicts disappearance of the center fixation which served as a cue (C) for participants to freely view the four stimuli (screen 4). Finally, participants reported the amount of detected faces in each trial (screen 5). c. The Control condition started with a fixation on the screen center. Then, an arrow cue (C – screen 2) indicated the destination to which participants should perform a saccade (screen 3). Following the fixation (F1), stimulus appearance (S) occurred at the new fixation point (screen 4). Finally, participants reported if the stimulus was an egg or a face (screen 5)

Finally, the *Control condition* was similar to the Cued-Viewing condition, except that the endogenous and exogenous cues appeared before the appearance of the stimuli, instructing the participants to move their gaze to the white dot. 750-1150ms later, two stimuli appeared for 500ms at the upper corners, one of which was centered at the participant's new fixation point. Thus, the control condition replicated the classical event-related paradigm in the sense that stimuli appeared where the eyes are fixating, but it did so while controlling for similar gaze position across the 3 conditions. The behavioral task was again to indicate whether the cued stimulus was a face or not.

The 3 conditions were blocked, and their order was counterbalanced across participants. In each condition there were about 300 trials divided into 5 runs separated by a rest period. The number of faces and eggs presented in a trial were counter balanced across trials and the stimuli randomly chosen from the pool of faces or eggs accordingly. They were presented at the corners of the screen such that their distance from the fixation symbol was $\sim 8°$. The location and size of the stimuli were piloted to prevent para-foveal classification of the stimulus as containing an egg or a face before preforming a saccade to the stimulus. Each condition was preceded by detailed instructions and a practice session of 20 trials.

EEG and Eye-tracking co-registration

EEG was acquired using an Active 2 system (Biosemi, The Netherlands) from 64 electrodes mounted on an elastic cap according to the extended 10–20 system, at a sampling rate of 512Hz. Eight additional electrodes were placed: two on the mastoid processes, two horizontal EOG electrodes positioned at the outer canthi of the left and right eyes, two vertical EOG electrodes, one below and one above the right eye, a single EOG channel placed under the left eye, and a channel on the tip of the nose. All electrodes were referenced during recording to a common-mode signal (CMS) electrode between POz and PO3, and an online low-pass filter with a cutoff of 1/5 of the sampling rate was applied to prevent aliasing.

Binocular eye movements were recorded using a desktop mount Eyelink 1000/2K infrared video-oculography system (SR Research Ltd., Ontario, Canada), at a rate of 500 Hz. A 9- point calibration procedure was applied before every experimental condition. A gaze drift check was performed after every 10 trials and a calibration procedure was repeated every block or if necessary. Triggers sent via a parallel port from the stimulation computer were split and recorded simultaneously by the EEG recording system and by the eye tracker, allowing offline synchronization between the records. Eye position and pupil data generated by the Eyelink system were also recorded by the Biosemi system as additional analog channels. This was used to ensure correct synchronization but the analysis was performed on the digital data recorded by the eye tracker, which has better SNR.

Eye movement data analysis

Analysis was performed on the participants' dominant eye. Saccades and fixations were detected using the Eyelink propriety algorithm which identifies when the moment-to-moment velocity and acceleration of the eye exceeds a pre-determined threshold velocity of $\frac{30°}{\text{sec}}$, an acceleration of $\frac{8000°}{\text{sec}^2}$, and a minimum position change threshold of 0.1°.[2] Exclusion criteria for detected saccades were: 1) If a blink occurred during the saccade, 2) If the saccade amplitude exceeded the diagonal screen size ($> 28°$) or 3) If the saccade duration was longer than 100ms, which is unlikely. Fixations were excluded if their duration was longer than 2.5 sec, if they occurred within 20ms of a blink, or if they followed an invalid saccade according to the above criteria. We verified that the difference between a detected saccade offset and its ensuing fixation onset was no more than 4ms. On average, ~1.2% of fixations were removed per participant due to these exclusion criteria. These events were kept for consideration in the regression analysis (see

[2] Saccade detection was qualitatively verified by comparison to the Engbert et al. paradigm (Engbert & Kliegl, 2003). Note that the fixations analyzed in this study follow macro- rather than micro-saccades.

Regression Fixation Related Potentials) but were marked as invalid events. Blinks were defined from 5ms before the eye tracker lost gaze location to 5 ms after gaze was reestablished.

The onset of fixations was defined as the end of the preceding saccades, based on predetermined criteria for a saccade (using the Eyelink algorithm, see above) or based on the statistics of eye-movement velocity (Engbert & Kliegl, 2003). Note that these parameters might not be optimal for every fixation in the data. To test whether this uncertainty in the definition of the fixation onset affected the results, we performed a second step of fixation-realignment, based on the local movement statistics around each fixation separately. This was done by defining a window of $\pm 100ms$ around the fixation onset, that was further constrained by including only one preceding saccade. We then corrected the fixation onset to be the first point to cross below 2 standard deviations of the eye velocity data. This resulted in realigning the fixations to the end of the main saccadic movement (see Supplementary 1). The FRPs were hardly affected by the different onset definitions.

Fixations of interest (FOIs) were detected within the stimuli region of interest (ROI). The ROI was defined as the area within the external frame of the object picture (Figure 1). We chose this ROI definition after we verified that fixations within this frame were sufficient for the participants to accurately report the object identity. A valid "first fixation" (F1) in the Cued- and Uncued-viewing conditions was the first fixation within the ROI of a stimulus which followed a saccade larger than at least $\sim 6°$ visual degrees. This ensured that a previous fixation, if happened, was far enough from the stimulus to prevent para-foveal identification. Fixations occurring within 20 ms from a blink, or during EEG artifacts, were marked as invalid fixations and were modeled separately (see below). Overall 7% of fixations were considered invalid. We verified that for each subject a similar amount of trials for Face and Egg stimuli were included in all three conditions (supplementary 3).

EEG pre-processing

Data processing was done with custom Matlab code (Mathworks, Natick, MA), with some functionality adopted from the Fieldtrip toolbox (Oostenveld et al., 2011) and the EEGLab toolbox (Delorme & Makeig, 2004). Electrodes that included excessive noise across the entire experiment duration (based on visual inspection) were excluded (1-2 channels in 4 out of 12 participants), and recreated by mean interpolation of the neighboring electrodes, after the pre-processing stage was completed. All EEG data was re-referenced to an average of 56 (excluding the excluded noisy electrodes) out of the 64 scalp electrodes, excluding the 8 most frontal electrodes (Fp1,2,z and AF7,3,z,4,8), which are most sensitive to eye movements. The data was high-pass filtered with a cutoff of 0.1 Hz with a 3rd degree, zero phase-shift

Butterworth filter, and 50Hz line noise was removed with a custom notch filter designed to suppress continuous 50 Hz oscillations, typical of power lines noise, while having less effect on more transient components (Keren et al., 2010). To avoid edge artifacts during filtering, each continuous recording block was individually de-trended prior to the filtering stage, by subtracting the linear vector connecting the means of the initial and final 10 samples of the block and the de-trended blocks were concatenated back together. To attenuate noise driven by eye movements and muscle activity, independent component analysis (ICA) was applied (as described in Keren et al., 2010). ICA training data was generated by concatenating segments of -500 to +1000 ms around stimuli onsets as well as -30 to +30 ms segments centered on every saccade-onset event (Engbert & Mergenthaler, 2006; Keren et al., 2010). ICA components were manually identified as reflecting ocular noise based on their temporal profile, scalp topography, power spectrum, and low-frequency power modulation around blinks, saccades or stimulus onsets. To remove noise components, these components were multiplied by zero and the data was then re-mixed into channel data. Next, extreme-value artifacts were semi-automatically identified using a threshold value of 100 µV together with visual inspection, and windows of $\pm$40 ms around the artifacts were excluded from analysis.

Regression Fixation Related Potentials

A time-resolved multiple regression model was applied directly to the continuous EEG data, in order to disentangle (de-convolve) the overlapping event-related responses to multiple events occurring in a semi-controlled manner in each trial (Smith & Kutas, 2015a, 2015b). We defined four temporally adjacent events within a trial for which we wanted to model a separate waveform: 1. Stimulus appearance (S); 2. Cue appearance (in Cued-viewing and control conditions) or disappearance (in the Uncued-viewing condition) (C); 3. First fixation on the stimulus (or the white dot in the control block) (F1); 4. Second immediate fixation on the stimulus (F2). The sequence of events for each block (see figure 1) was therefore: $S \rightarrow C \rightarrow F1 \rightarrow F2$ for the Cued and Uncued-viewing blocks, and $C \rightarrow F1 \rightarrow S \rightarrow F2$ in the control block. The response evoked by each event was modeled time-point by time-point over a window of 2000 ms (-200 to +1800ms) sampled at 512Hz, which resulted in total of 1024 data points. We define dummy coded predictors (or stick functions) $X_{event\ n\ ,latency\ l}$ that are 1 for data points measured at a specific latency l relative to the time-locking event n and 0 otherwise. In our model we therefore have $l = 1024$ data points and n=4 events of interest resulting in a total of 1024*4 predictors in the model. If l_2 is an index that runs on all latencies of interest around an event onset, the predictor for a specific latency l_1 will be 1 only when $l_1 = l_2$ and zero otherwise (equation 1).

1. $X_{event\ n\ ,latency\ l_1\ @\ trial\ i\ ,latency\ l_2} = f(x) = \begin{cases} X_{event\ n\ ,latency\ l_1\ @\ trial\ i}, & l_1 = l_2 \\ 0, & Otherwise \end{cases}$

Thus, each measured data point is modeled as a sum of the effects of overlapping event-related time series (equation 2):

2. $y_t = \beta_{n1,l1} * X_{n1,l1} + \cdots + \beta_{n1,l1024} * X_{n1,l1024} + \cdots + \beta_{n4,l1} * X_{n4,l1} + \cdots + \beta_{n4,l1024} * X_{n4,l1024}$

For example, for a series of events in the cued-viewing conditions (figure 1), voltage y recorded 600ms past stimulus onset (S), 300ms past arrow cue onset (C), 100ms past first fixation onset (F1), and before a second fixation (F2) the regression equation would be (equation 3):

3. $y = \beta_{S,l\neq 600} * 0 + \beta_{S,l=600} * 1 + \beta_{C,l\neq 300} * 0 + \beta_{C,l=300} * 1 + \beta_{F1,l\neq 100} * 0 + \beta_{F1,l=100} * 1 + \beta_{F2,\forall l} * 0$

Whereas the analysis was carried out in Matlab, the regression stage was run in Python, as it proved to handle the memory load required more efficiently than Matlab.

In addition to the binary event regressors, we included in the model a continuous-variable predictor of the saccade amplitude preceding a fixation, expanded over 5 spline basis functions (Ehinger & Dimigen, 2018), to account for the non-linear effect saccade size has on the lambda peak (Dandekar et al., 2012b; Dimigen et al., 2009; Ries et al., 2018). We removed from the continuous data (thus from the design matrix) any data points defined as artifacts. The regression procedure resulted in 'regression ERPs\FRPs' (rERPs in the Control condition, rFRPs in the Cued and Uncued-viewing conditions), which are the time-series of estimated coefficients per event. rERPs\rFRPs were then averaged over participants and baseline-corrected by subtracting the average of 200ms before the event of interest. For convenience, going forward we drop the 'r' prefix and refer to FRPs and ERPs.

Time windows with significant differences between the conditions were tested using a cluster permutation algorithm (Maris & Oostenveld, 2007). In this procedure, a time point by time point one-tailed t test between the response to faces and eggs was conducted, testing the hypothesis that the response to faces was more negative than for eggs. t values which crossed a threshold of an uncorrected level of $p<0.05$ were chosen, and sequential significant time points were clustered. For each cluster, the sum of the t (t_sum) values was determined. Next, to define the distribution of t_sum under the null hypothesis of no differences the same procedure was repeated 10,000 times, where in each iteration the

assignment of data to face or egg was permuted randomly, and the maximal t_sum value was recorded. Finally clusters in the original analysis with t_sum > the 95% percentile of t_sums in the null distribution were considered as significant. N170 effect peaks were defined as the peak negativity within the time window of 120-280 ms (large window around the N1).

Results

Behavioral Results

Participants were highly accurate in performing the behavioral tasks: detecting faces or eggs in the control and the cued-viewing task (control: hit rate *M* = .88, *SD* = .05; Cued-viewing: *M* = .91, *SD* = .03), and counting the number of faces in the Uncued-viewing block (correct count *M* = .85, *SD* = .09).

FRPs compared to ERPs

The main goal of this study was to compare the free-viewing N170 effect to the classical N170 face effect in time and space. We thus compared activity for faces vs. eggs (our non-face control stimulus) in 3 different conditions: Cued-viewing, Uncued-viewing, and control. Note that in all 3 conditions, the gaze direction was similarly deviated relative to the head. We first verified that we obtained the N170 effect in our control condition. Indeed, we observed a significantly larger negativity for faces compared to eggs peaking around 170ms. The topography of the "N170 effect" (the difference between faces and egg responses) was also consistent with previous studies, with a maximum at lateral temporo-occipital electrodes (N170; Bentin et al., 1996) and a concomitant frontal positivity (vertex positive potential or VPP (Joyce & Rossion, 2005;figure 2). Critically, in both of the FRP conditions (Cued and Uncued), we obtained a clear N170 face-specific effect, namely, the response to faces was significantly more negative than eggs at the expected latency of around 170ms (figure 2A,B).

The peak of the N170 effect smaller in amplitude and later in time for the FRPs (Cued and Uncued conditions) relative to the ERPs (control condition – figure 2B). A repeated-measure one-way analysis of variance (rmANOVA) of the N170 effect peak amplitude across conditions showed a marginally significant effect ($F(2,33) = 3.23$, $p = 0.052$). Although this is strictly a null result, we followed it up by planned comparisons of the ERPs (control condition) against the FRPs (Cued and Uncued conditions): the ERP N170 effect in the control condition elicited a larger negativity than the two FRPs combined ($t(11) = 3.66$, $p = 0.003$), while the two FRPs did not significantly differ ($t(11) = 1.37$, $p = 0.2$). Figure 2D depicts these

differences by comparing the single subject peak amplitudes in the Control vs Cued conditions (top left) where most subjects show larger peak amplitudes in the control condition, while those in the Cued vs Uncued conditions are mostly similar (top right). A similar rmANOVA for peak latency of the N170 effect found a significant effect of condition ($F(2,33) = 4.12$, $p = 0.025$); follow up tests showed that the latency of the ERP was significantly earlier than that of the two FRPs combined ($t(11) = -4.3$, $p = 0.001$), while the difference between the two FRP latencies was not significant statistically ($t(11) = 0.2$, $p = 0.84$). Again these differences can be seen in single subject data (figure 2D-bottom). The differences in amplitude and latency remained similar whether we used the fixation times based on the propriety Eyelink definitions or if we further realigned fixation onsets (see methods).

Scalp distributions

The scalp topography of the N170 differential effect at its peak latency showed similar distribution across conditions (figure 2.C, top row). However, this was not the case for the responses to faces and eggs separately (figure 2.C, bottom). Broadly, for both faces and eggs, fixation related responses were dominated by a midline occipital positivity and concomitant frontal negativity, whereas event related responses showed a central-frontal positivity accompanied by occipito-temporal negativity (figure 2.C, bottom). Next, we examine these differences in more detail.

[figure 2 about here]

Fig. 2 Comparison of the ERP and FRP face effect. A. the grand average regression ERPs/FRPs obtained by Egg stimuli and Face stimuli separately for each experimental condition and the difference waves depicting the face effect. Windows of significant difference marked based on cluster permutation statistics for $p<0.05$. B. Faces-Eggs difference wave in all three blocks superimposed with a 95% confidence interval depicted by the shaded error-bars. C. Scalp distributions averaged over a window of 30ms around the N1 peak latency, per condition. D. Single subject N170 peak amplitudes (top) and latencies (bottom) compared between conditions – Cued vs Control (left) and Cued vs Uncued (right)

Figures 3 and 4 depict the evolution in time of the activity elicited by eggs, faces and the face-egg difference, for each condition. The first difference between the viewing conditions emerges during the P1 peak (100ms). While the positive voltage at lateral occipito-temporal electrodes (P9\P10) is evident for all conditions (figure 2.B, figure 3), a central occipital positivity starting as early as 80ms and accompanied by a frontal negativity is seen for the FRPs (Cued- and Uncued alike), but not for the ERPs (control condition). In the N1 window, the ERP induced by face stimuli shows a clear N1 peak (~170 ms) in medial occipital as well as stronger negativity in lateral temporo-occipital electrodes, and a positive counterpart in the fronto-central electrodes (vertex positive potential, VPP). In contrast, the FRPs (Cued and Uncued conditions) show no N1 in medial occipital electrodes nor its positive counterpart in frontal electrodes.

However, occipital-temporal (P9\P10) electrodes show a clear N1 deflection (~190ms) in these conditions. Taken together, these results show that while the category selective activity (face-egg) is topographically similar whether locking the neural signal to stimulus onset or fixation onset, the overall neuronal signals elicited by each category on its own are different between the two viewing conditions.

[figure 3 about here]

Fig.3 Development in time of the response to faces (a), eggs(b) and to the face-egg difference wave(c). The Lambda component in the FRPs starts earlier than P1 of the ERP and is more "spread out" including central occipital electrodes. The occipital component is sustained in the FRPs. N1 peaks later in the FRPs

[figure 4 about here]

Fig.4 ERPs\FRPs of the response to faces in a subset of the electrodes. The red and green vertical lines indicate the P1 and N1 peaks respectively. While the Central and Parietal electrodes (P9\10, Cz, Pz) electrodes show similar waveforms, the main differences emerge in the Occipital and Frontal electrodes (F1\z\2, O1\z\2). For similar results in response to eggs, see supplementary 1

What could be the reason for the striking difference in the scalp recorded responses between ERPs and FRPs, a difference that nevertheless preserves a similar face-effect? One explanation could be that the initial P1\lambda activity, which is different for a stimulus versus a fixation onset (Yagi, 1979), may overlap with the categorical processing reflected by the occipito-parietal N1. To test the plausibility of this hypothesis, we simulated the development in time of possible dipole sources using the Brain Electrical Source Analysis (BESA) software (MEGIS Software GmbH, Gräfelfing, Germany). Note that this simulation was not an exploratory source localization ("inverse solution") analysis, but rather a confirmatory "forward" solution analysis designed to test a hypothesis. That is, we seeded dipoles in hypothetical locations based on previous dipole localization literature, and with hypothetical time courses, and examined the resulting scalp distribution over time. First, the "face effect" was modeled by two transient dipoles starting around 90ms and peaking around 170ms, located in right\left occipital-temporal cortex (roughly Brodmann areas 37 of the posterior fusiform gyrus) (Bentin et al., 1996; Di Russo et al., 2002; Itier & Taylor, 2004).

[figure 5 about here]

Fig.5 Source model using BESA simulator. a- The Spatial organization of the dipoles used in the model. b- Position of the modeled dipoles in Talairach coordinates. c- The dynamics of each dipole. P1\lambda dipoles have a nonsymmetrical dynamics and peak at 90ms, N1 dipoles peak at 170

Next, we added two lateralized dipoles modeling the P1 activity located in the visual association area in the extra-striate cortex (roughly Brodmann 18\19) (Clark et al., 1995; Mangun, 1995; Martínez et al., 1999) oriented towards the midline, starting around 60ms and peaking around 100ms with slowly decaying sustained activity (figure 5.A-B). This seems plausible as Di Russo et al., (2002) have reported an overlap of the N1 and P1 sources in VEPs. This configuration of 4 dipoles peaking at two different time points simulated the ERP condition topography in the control condition (figure 6). The difference between the ERP topography and the FRP topographies could be captured by adding a single dipole over the Calcarine sulcus with posterior\anterior orientation (figure 5.A-C), previously suggested as the location of the lambda complex generator, which is activated upon a new fixation (Kazai & Yagi, 2003). This additional dipole causes a reversal in the FRP components in the occipital and frontal electrodes compared to the control ERPs, hardly effecting the FRP component orientations in occipital-parietal electrodes (P9/P10) (figure 6), as seen in the experimental data.

[figure 6 about here]

Fig.6 Simulated topographies (a) and waveforms (b). The classic control ERP is modeled using 4 diploes (figure 5) reflecting the P1 and N1. The Cued condition FRP is modeled by adding the "lambda" dipole. The red and green vertical lines indicate the P1 and N1 peaks respectively as in figure 4

Discussion

Traditional studies of visual perception rely mainly on a serial presentation of stimuli at the center of the visual field, while the viewer tries to keep his or her gaze fixed. Such well-controlled paradigms have obvious methodological benefits, but they are quite removed from real-life perception. In real-life, stimuli do not appear abruptly out of the void, and viewers are free to search and scan, as well as benefit from prior background (peripheral) information. The overall goal of using fixation-related, rather than event-related, potentials is to study visual cognition while taking into account the dynamics of natural vision and the possible role that active sampling has on perception. The focus of the current study was on a well-known signature of category selective processing, the N170 effect, and its manifestation in fixation-related Potentials using EEG and Eye movements co-registration, as compared to the traditional way of presenting stimuli serially at fixation. This would be an essential step towards bridging the gap between perception in more natural viewing, what we know about categorical perception from artificial laboratory experiments.

We demonstrated that the N170 effect, that is, the difference between the response to faces and non-face stimuli, is clearly apparent when locking EEG activity to fixation on a peripheral stimulus, with a similar topography to that found using ERPs generated by stimulus onset at fixation point. This establishes the use of the N170 effect as a signature of face (vs. non-faces) detection in free viewing experiments. The FRP N170 effect was of slightly smaller amplitude and longer latency than that of the ERP effect. The longer latency is consistent with the result of a very recent study using face stimuli with FRPs, although that study did not address the face-effect *per se* as no non-face stimuli were presented (Huber-Huber et al., 2019). In addition, there was no direct comparison to ERPs (ERPs in that study were limited to peripheral stimuli and showed even later N1). We cannot rule out the possibility that the differences between the N170 effect in FRP versus ERP are a consequence of the inherently less determined moment of fixation onsets as compared to the well-determined timing of the stimulus onset. That said, our attempts to realign the fixations had a very small effect on the results (see methods and sup.3). Future studies should further investigate this slight amplitude and latency difference.

While the ERP and FRP differential face-effect showed overall similar components and topographies (figure 2), differences between ERPs and FRPs were prominent within each category separately (figure 2.C, 3 and 4). Specifically, ERP and FRP topographic differences emerged both around ~100ms (P1\lambda components) and around ~170 ms (N1 component) from stimulus or fixation onset (figure 3 and 4). Two fundamental distinctions between the event-related paradigm and active vision situation might account for this. First, in event-related paradigms there is a local external change in the visual field, while in free viewing there are changes across of the whole visual field following the eye movement. Second, since the saccade is self-generated (even if cued), free viewing may not only utilize peripheral information to predict the input (Huber-Huber et al., 2019), but also generate precise temporal predictions. These differences might affect components associated with both high and low-level feature processing. We next discuss the major topographical dissimilarities and the implications on our understanding of the ERP and FRP components.

P1 component

In visual evoked potentials, the P1 component is a positive deflection peaking around 100 ms after stimulus onset, maximal over occipital electrodes. It is commonly thought to reflect low-level feature processing that can be modulated by spatial attention (Hillyard and Anllo-Vento, 1998,). The P1 component could be related the to the lambda response, a well-known component locked to fixation onset, with a positive peak largest at occipital sites and reversed polarity in frontal electrodes, with a peak

latency ~100 ms (Dimigen et al., 2011; Kazai & Yagi, 2005; Thickbroom, Knezevič, Carroll, & Mastaglia, 1991; Yagi, 1981). Similar to the P1 component, the lambda response is modulated by low level features such as luminance, size and contrast (Tobi- matsu & Celesia, 2006). Based on these similarities between the P1 in a pattern-reversal paradigm and the lambda response, a common generator for these components has been suggested (Kazai & Yagi, 2003). In our study, however, the topography of the ERP P1 component and the FRP lambda response were quite different. The FRP lambda response started earlier and was maximal in central occipital electrodes (O1/O2), where the ERP P1 was very small if at all noticeable. The event-related P1 component was maximal in lateral occipito-temporal electrodes (P9/P10) and was of the same amplitude and latency as the fixation-related lambda response in these electrodes. These results do not necessarily contradict the possibility that there are common generators for these two components. In the study of Kazai & Yagi, (2003), ERPs were generated by a full screen checkerboard pattern reversal, and were compared to FRPs generated by alternate fixations on two points on the background of the same checkerboard. Presumably, the spatial extent of retinal change was similar in the two conditions. In our experiment, in contrast, the change in the retinal image in the control condition (ERPs) occurred foveally, namely, within a radius of about 2 visual degrees, whereas in the FRPs conditions, saccades of about 8 visual degrees to the peripheral images caused an entire shift of the retinal image. The activation of a broader population of neurons responding to such a change could explain the wider distribution of the lambda response compared to the P1, requiring, in our simulation, an additional midline dipole.

N1 component

Face processing ERP literature focuses mainly on the major negative deflection (N1) in ocipito-temporal sites (Bentin et al., 1996; Bentin & Golland, 2002), or its positive counterpart (VPP) at centro-frontal sites (Jeffreys, 1996; Joyce & Rossion, 2005), ~170 ms post stimulus onset. As mentioned above, we identified the N170 face specific component (subtraction of face-egg) with similar time course and topographies in all experimental conditions (ERPs and FRPs). Nevertheless, the N1 topography for each category separately differed between the experimental conditions. In the ERP paradigm, the N1 was maximal in lateral occipito-temporal electrodes (P9/P10) but was observed in all occipital electrodes, with a positive counterpart in frontal electrodes. In contradistinction, the N1 peak of the FRPs was limited to the occipito-temporal electrodes, with no spread to the occipital electrodes, and with no positive counterpart in the frontal electrodes. As shown by the dipole simulation (figures 5-6) this could be explained by temporal overlap of the N1 component with the strong midline occipital activity generated by an equivalent dipole with an anterior-posterior orientation (ascribed above to the lambda response).

Conclusions

Here, we demonstrate that category specific processing can be tracked in free-viewing conditions using co-registration of Eye-Movements and EEG, by time-locking the activity to the first fixation on an object and disentangling activity overlap with previous and ensuing saccades. We showed that this category-specific activity is highly similar for FRPs and ERPs, provided that an appropriate contrast is used to eliminate non-specific response. Nevertheless, the interpretation of FRPs to specific categories should take into account the potential interaction of the sensory or cognitive process in question with the strong evoked lambda complex generated by the fixation onset. As was done over the decades for ERPs, better understanding of fixation-specific responses will allow a better interpretation of experimental effects as well as modelling of overlapping responses.

Ethical approval: All procedures performed in studies involving human participants were in accordance with the ethical standards of the institutional and/or national research committee (include name of committee + reference number) and with the 1964 Helsinki declaration and its later amendments or comparable ethical standards.

References

Amihai, I., Deouell, L. Y., & Bentin, S. (2011). Neural adaptation is related to face repetition irrespective of identity: A reappraisal of the N170 effect. *Experimental Brain Research*, *209*(2), 193–204. https://doi.org/10.1007/s00221-011-2546-x

Baccino, T., & Manunta, Y. (2005). Eye-fixation-related potentials: Insight into parafoveal processing. *Journal of Psychophysiology*, *19*(3), 204–215. https://doi.org/10.1027/0269-8803.19.3.204

Bentin, S., Allison, T., Puce, A., Perez, E., & McCarthy, G. (1996). Electrophysiological Studies of Face Perception in Humans. *Journal of Cognitive Neuroscience*, *8*(6), 551–565. https://doi.org/10.1162/jocn.1996.8.6.551

Bentin, S., & Golland, Y. (2002). Meaningful processing of meaningless stimuli: The influence of perceptual experience on early visual processing of faces. *Cognition*, *86*(1). https://doi.org/10.1016/S0010-0277(02)00124-5

Brouwer, A.-M., Reuderink, B., Vincent, J., van Gerven, M. A. J., & van Erp, J. B. F. (2013). Distinguishing between target and nontarget fixations in a visual search task using fixation-related potentials. *Journal of Vision*, *13*(3), 17–17. https://doi.org/10.1167/13.3.17

Clark, V. P., Fan, S., & Hillyard, S. A. (1995). Identification of early visual evoked potential generators by retinotopic and topographic analyses. *Human Brain Mapping*, *2*(3), 170–187. https://doi.org/10.1002/hbm.460020306

Dandekar, S., Privitera, C., Carney, T., & Klein, S. a. (2012). Neural saccadic response estimation during natural viewing. *Journal of Neurophysiology*, *107*(6), 1776–1790. https://doi.org/10.1152/jn.00237.2011

Delorme, A., & Makeig, S. (2004). EEGLAB: an open source toolbox for analysis of single-trial EEG dynamics including independent component analysis. *Journal of Neuroscience Methods*, *134*(1), 9–21. https://doi.org/10.1016/j.jneumeth.2003.10.009

Devillez, H., Guyader, N., & Guérin-Dugué, A. (2015). An eye fixation–related potentials analysis of the P300 potential for fixations onto a target object when exploring natural scenes. *Journal of Vision*, *15*(13), 20. https://doi.org/10.1167/15.13.20

Di Russo, F., Martínez, A., Sereno, M. I., Pitzalis, S., & Hillyard, S. A. (2002). Cortical Sources of the Early Components of the Visual Evoked Potential. *Human Brain Mapping*, *15*(2), 95–111. https://doi.org/10.1002/hbm.10010

Dimigen, O., Sommer, W., Hohlfeld, A., Jacobs, A. M., & Kliegl, R. (2011). Coregistration of eye movements and EEG in natural reading: Analyses and review. *Journal of Experimental Psychology: General*, *140*(4), 552–572. https://doi.org/10.1037/a0023885

Dimigen, O., Valsecchi, M., Sommer, W., & Kliegl, R. (2009). Human Microsaccade-Related Visual Brain Responses. *Journal of Neuroscience*, *29*(39), 12321–12331. https://doi.org/10.1523/JNEUROSCI.0911-09.2009

Ehinger, B. V., & Dimigen, O. (2018). Unfold: An integrated toolbox for overlap correction, non-linear modeling, and regression-based EEG analysis. *BioRxiv*, 360156. https://doi.org/10.1101/360156

Engbert, R., & Kliegl, R. (2003). Microsaccades uncover the orientation of covert attention. *Vision Research*, *43*(9), 1035–1045. https://doi.org/10.1016/S0042-6989(03)00084-1

Engbert, R., & Mergenthaler, K. (2006). Microsaccades are triggered by low retinal image slip. *Proceedings of the National Academy of Sciences of the United States of America*, *103*(18), 7192–7197. https://doi.org/10.1073/pnas.0509557103

Fischer, T., Graupner, S. T., Velichkovsky, B. M., & Pannasch, S. (2013). Attentional dynamics during free picture viewing: Evidence from oculomotor behavior and electrocortical activity. *Frontiers in Systems Neuroscience*, *7*(17), 1–9. https://doi.org/10.3389/fnsys.2013.00017

Frey, A., Ionescu, G., Lemaire, B., López-orozco, F., Baccino, T., & Guérin-dugué, A. (2013). Decision-making in information seeking on texts : an eye-fixation-related potentials investigation. *Frontiers in systems neuroscience*, *7*, 39. https://doi.org/10.3389/fnsys.2013.00039

Henderson, J. M., Williams, C. C., & Falk, R. J. (2005). Eye movements are functional during face learning. *Memory and Cognition*, *33*(1), 98–106. https://doi.org/10.3758/BF03195300

Hillyard, S. a, & Anllo-Vento, L. (1998). Event-related brain potentials in the study of visual selective attention. *Proceedings of the National Academy of Sciences of the United States of America*, *95*(3), 781–787. https://doi.org/10.1073/pnas.95.3.781

Hsiao, J. H. W., & Cottrell, G. (2008). Two Fixations Suffice in Face Recognition. *Psychological Science*, *19*(10), 998–1006. https://doi.org/10.1111/j.1467-9280.2008.02191.x

Huber-Huber, C., Buonocore, A., Dimigen, O., Hickey, C., & Melcher, D. (2019). The peripheral preview effect with faces: Combined EEG and eye-tracking suggests multiple stages of trans-saccadic predictive and non-predictive processing. *NeuroImage*, *200*(May), 344–362. https://doi.org/10.1016/j.neuroimage.2019.06.059

Hutzler, F., Braun, M., Võ, M. L. H., Engl, V., Hofmann, M., Dambacher, M., … Jacobs, A. M. (2007). Welcome to the real world: Validating fixation-related brain potentials for ecologically valid settings. *Brain Research*, *1172*(1), 124–129. https://doi.org/10.1016/j.brainres.2007.07.025

Itier, R. J., & Taylor, M. J. (2004). Source analysis of the N170 to faces and objects. *NeuroReport*, *15*(8), 1261–1265. https://doi.org/10.1097/01.wnr.0000127827.73576.d8

Jeffreys, D. A. (1996). Evoked Potential Studies of Face and Object Processing. *Visual Cognition*, *3*(1), 1–38. https://doi.org/10.1080/713756729

Joyce, C., & Rossion, B. (2005). The face-sensitive N170 and VPP components manifest the same brain processes: The effect of reference electrode site. *Clinical Neurophysiology*, *116*(11), 2613–2631. https://doi.org/10.1016/j.clinph.2005.07.005

Kamienkowski, J. E., Ison, M. J., Quiroga, R. Q., & Sigman, M. (2012). Fixation-related potentials in visual search: A combined EEG and eye tracking study. *Journal of Vision*, *12*(7), 4–4. https://doi.org/10.1167/12.7.4

Kaunitz, L. N., Kamienkowski, J. E., Varatharajah, A., Sigman, M., Quiroga, R. Q., & Ison, M. J. (2014). Looking for a face in the crowd: Fixation-related potentials in an eye-movement visual search task. *NeuroImage*, *89*, 297–305. https://doi.org/10.1016/j.neuroimage.2013.12.006

Kazai, K., & Yagi, A. (2003). Comparison between the lambda response of eye-fixation-related potentials

and the P100 component of pattern-reversal visual evoked potentials. *Cognitive, Affective and Behavioral Neuroscience*, *3*(1), 46–56. https://doi.org/10.3758/CABN.3.1.46

Kazai, K., & Yagi, A. (2005). Contrast dependence of lambda response. *International Congress Series*, *1278*, 61–64. https://doi.org/10.1016/j.ics.2004.11.053

Keren, A. S., Yuval-greenberg, S., & Deouell, L. Y. (2010). Saccadic spike potentials in gamma-band EEG : Characterization , detection and suppression. *NeuroImage*, *49*(3), 2248–2263. https://doi.org/10.1016/j.neuroimage.2009.10.057

Mangun, G. R. (1995). Neural mechanisms of visual selective attention. *Psychophysiology*, *32*(1), 4–18. https://doi.org/10.1111/j.1469-8986.1995.tb03400.x

Maris, E., & Oostenveld, R. (2007). Nonparametric statistical testing of EEG- and MEG-data. *Journal of Neuroscience Methods*, *164*(1), 177–190. https://doi.org/10.1016/j.jneumeth.2007.03.024

Martinez-Conde, S., Macknik, S. L., & Hubel, D. H. (2004). The role of fixational eye movements in visual perception. *Nature Reviews Neuroscience*, *5*(3), 229–240. https://doi.org/10.1038/nrn1348

Martínez, A., Anllo-Vento, L., Sereno, M. I., Frank, L. R., Buxton, R. B., Dubowitz, D. J., … Hillyard, S. A. (1999). Involvement of striate and extrastriate visual cortical areas in spatial attention. *Nature Neuroscience*, *2*(4), 364–369. https://doi.org/10.1038/7274

Meyberg, S., Sommer, W., & Dimigen, O. (2017). How microsaccades relate to lateralized ERP components of spatial attention: A co-registration study. *Neuropsychologia*, *99*, 64–80. https://doi.org/10.1016/j.neuropsychologia.2017.02.023

Min, X., Zhai, G., & Gu, K. (2015). Visual Attention on Human Face. *2015 Visual Communications and Image Processing (VCIP)* (pp. 1-4). IEEE. https://doi.org/10.1109/VCIP.2015.7457922

Nikolaev, A. R., Meghanathan, R. N., & van Leeuwen, C. (2016). Combining EEG and eye movement recording in free viewing: Pitfalls and possibilities. *Brain and Cognition*, *107*, 55–83. https://doi.org/10.1016/j.bandc.2016.06.004

Nikolaev, Jurica, Nakatani, Plomp, & Leeuwen, V. (2013). Visual encoding and fixation target selection in free viewing: presaccadic brain potentials. *Frontiers in Systems Neuroscience*, *7*, 26. https://doi.org/10.3389/fnsys.2013.00026

Oostenveld, R., Fries, P., Maris, E., & Schoffelen, J. M. (2011). FieldTrip: Open source software for advanced analysis of MEG, EEG, and invasive electrophysiological data. *Computational Intelligence and Neuroscience*, *2011*, 156869. https://doi.org/10.1155/2011/156869

Ries, A. J., Slayback, D., & Touryan, J. (2018). The fixation-related lambda response: Effects of saccade magnitude, spatial frequency, and ocular artifact removal. *International Journal of Psychophysiology*, *134*, 1–8. https://doi.org/10.1016/j.ijpsycho.2018.09.004

Rossion, B. (2014). Understanding face perception by means of human electrophysiology. *Trends in Cognitive Sciences*, *18*(6), 310–318. https://doi.org/10.1016/j.tics.2014.02.013

Rossion, B., Gauthier, I., Tarr, M. J., Despland, P., Bruyer, R., Linotte, S., & Crommelinck, M. (2000). The N170 occipito-temporal component is delayed and enhanced to inverted faces but not to inverted objects: an electrophysiological account of face-specific processes in the human brain. *NeuroReport*, *11*(1), 69–72. https://doi.org/10.1097/00001756-200001170-00014

Rousselet, G. A., Mace, M. J. M., & Fabre-Thorpe, M. (2004). Animal and human faces in natural scenes: How specific to human faces is the N170 ERP component? *Journal of Vision*, *4*(1), 2–2. https://doi.org/10.1167/4.1.2

Schroeder, C. E., Wilson, D. A., Radman, T., Scharfman, H., & Lakatos, P. (2010). Dynamics of Active Sensing and perceptual selection. *Current Opinion in Neurobiology*, *20*(2), 172–176. https://doi.org/10.1016/j.conb.2010.02.010

Smith, N. J., & Kutas, M. (2015a). Regression-based estimation of ERP waveforms: I. The rERP framework. *Psychophysiology*, *52*(2), 157–168. https://doi.org/10.1111/psyp.12317

Smith, N. J., & Kutas, M. (2015b). Regression-based estimation of ERP waveforms: II. Nonlinear effects, overlap correction, and practical considerations. *Psychophysiology*, *52*(2), 169–181. https://doi.org/10.1111/psyp.12320

Thickbroom, G. W., Knezevič, W., Carroll, W. M., & Mastaglia, F. L. (1991). Saccade onset and offset lambda waves: relation to pattern movement visually evoked potentials. *Brain Research*, *551*(1–2), 150–156. https://doi.org/10.1016/0006-8993(91)90927-N

Volkmann, F. C. (1986). Human visual suppression. *Vision Research*, *26*(9), 1401–1416. https://doi.org/10.1016/0042-6989(86)90164-1

Yagi, A. (1979). Lambda waves associated with offset of saccades: A subject with large lambda waves. *Biological Psychology*, *8*(3), 235–238. https://doi.org/10.1016/0301-0511(79)90051-6

Yagi, A. (1981). Visual signal detection and lambda responses. *Electroencephalography and Clinical Neurophysiology*, *52*(6), 604–610. https://doi.org/10.1016/0013-4694(81)91434-6

Yarbus, A. (1967). *Eye movements and vision*, Plenum Press, New York. https://doi.org/10.1016/0028-3932(68)90012-2

Figure 1

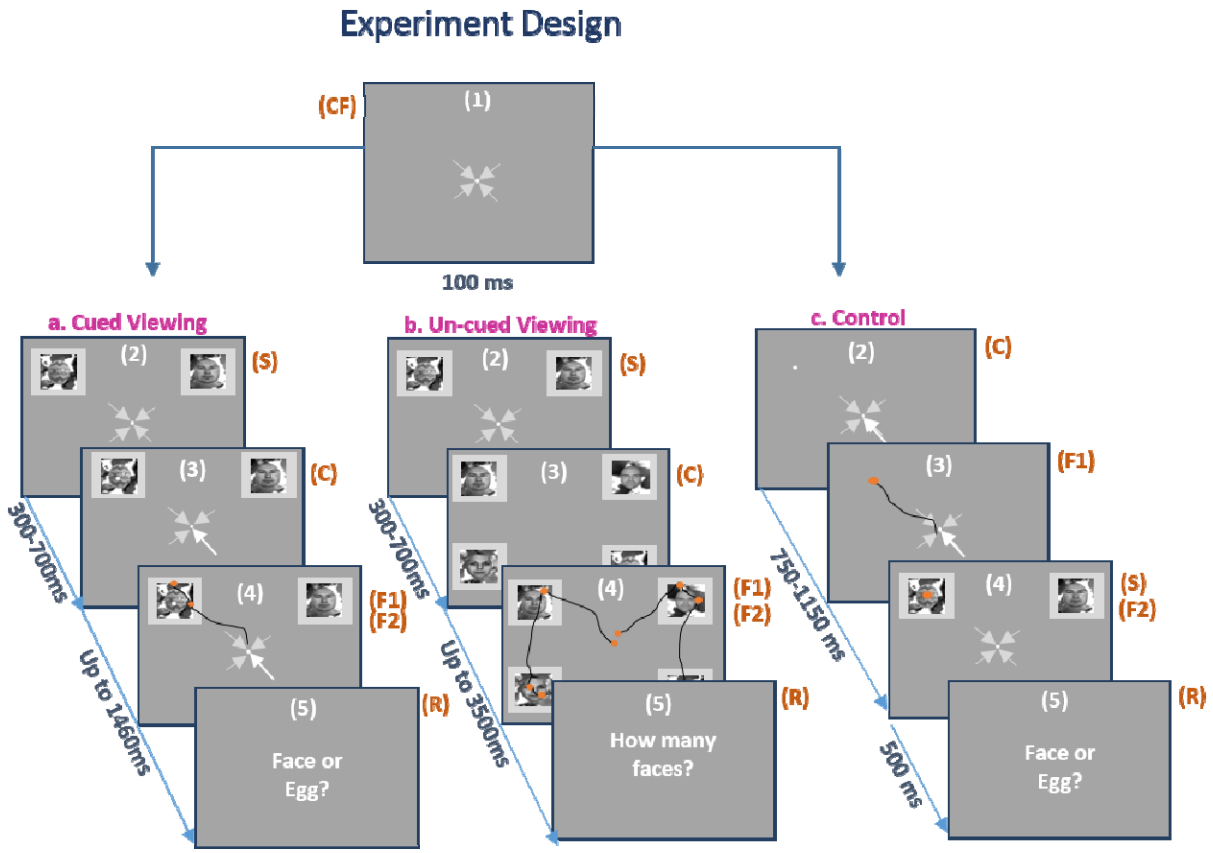
Experiment Design
(CF)
(1)
100 ms
a. Cued Viewing
(2)
(S)
(3)
(C)
(4)
(F1)
(F2)
(5)
(R)
Face or
Egg?
300-700ms
Up to 1460ms
b. Un-cued Viewing
(2)
(S)
(3)
(C)
(4)
(F1)
(F2)
(5)
(R)
How many
faces?
300-700ms
Up to 3500ms
c. Control
(2)
(C)
(3)
(F1)
(4)
(S)
(F2)
(5)
(R)
Face or
Egg?
750-1150 ms
500 ms

Figure 2

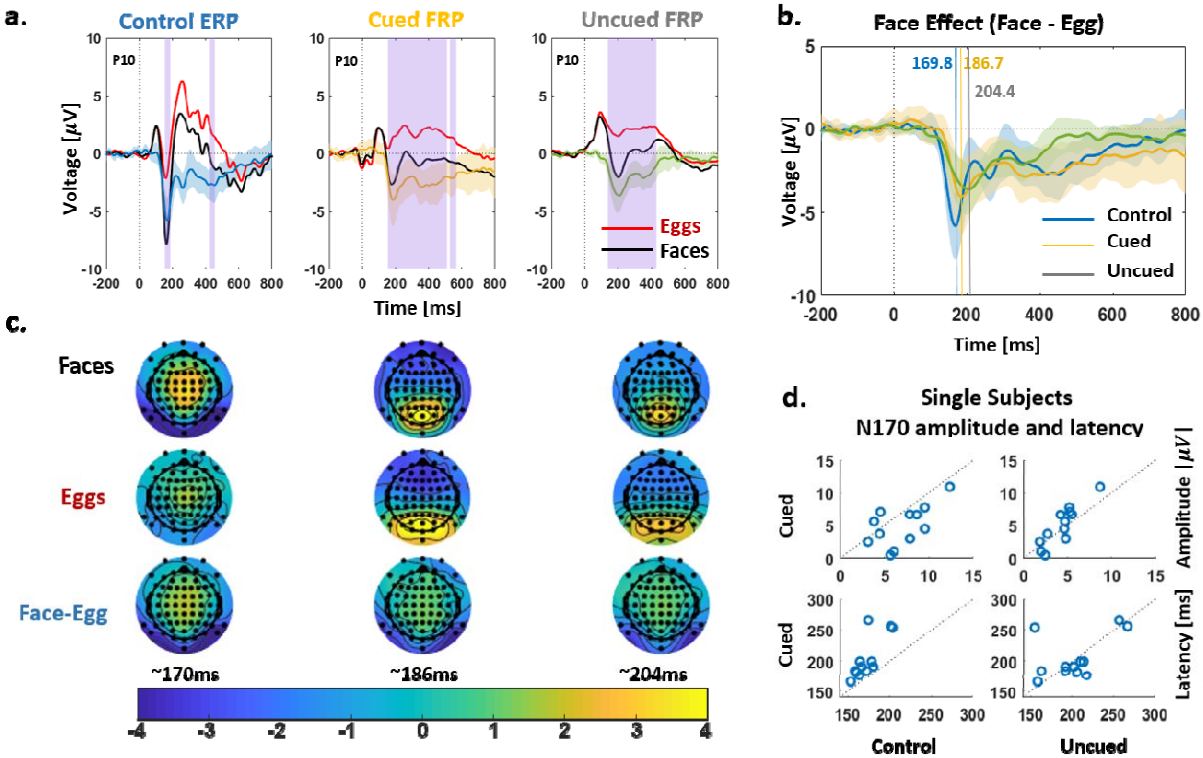
a.
Control ERP
Cued FRP
Uncued FRP
P10
Voltage [μV]
Time [ms]
Eggs
Faces
b.
Face Effect (Face - Egg)
169.8
186.7
204.4
Control
Cued
Uncued
Voltage [μV]
Time [ms]
c.
Faces
Eggs
Face-Egg
~170ms
~186ms
~204ms
d.
Single Subjects
N170 amplitude and latency
Cued
Control
Uncued
Amplitude [μV]
Latency [ms]

Figure 3

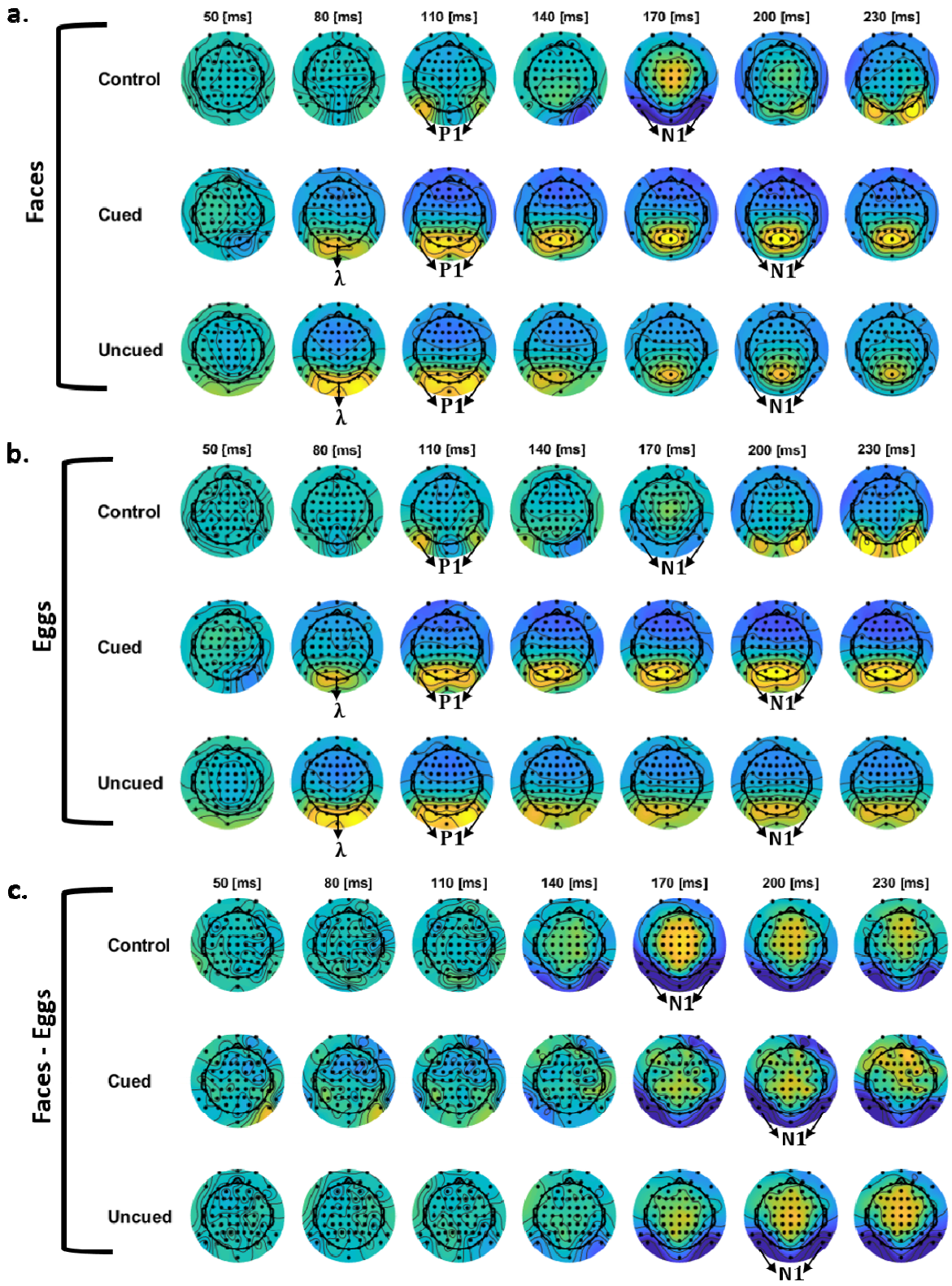
a.
Faces
Control
Cued
Uncued
50 [ms]
80 [ms]
110 [ms]
140 [ms]
170 [ms]
200 [ms]
230 [ms]
P1
N1
λ
b.
Eggs
Control
Cued
Uncued
50 [ms]
80 [ms]
110 [ms]
140 [ms]
170 [ms]
200 [ms]
230 [ms]
P1
N1
λ
c.
Faces - Eggs
Control
Cued
Uncued
50 [ms]
80 [ms]
110 [ms]
140 [ms]
170 [ms]
200 [ms]
230 [ms]
N1

Figure 4

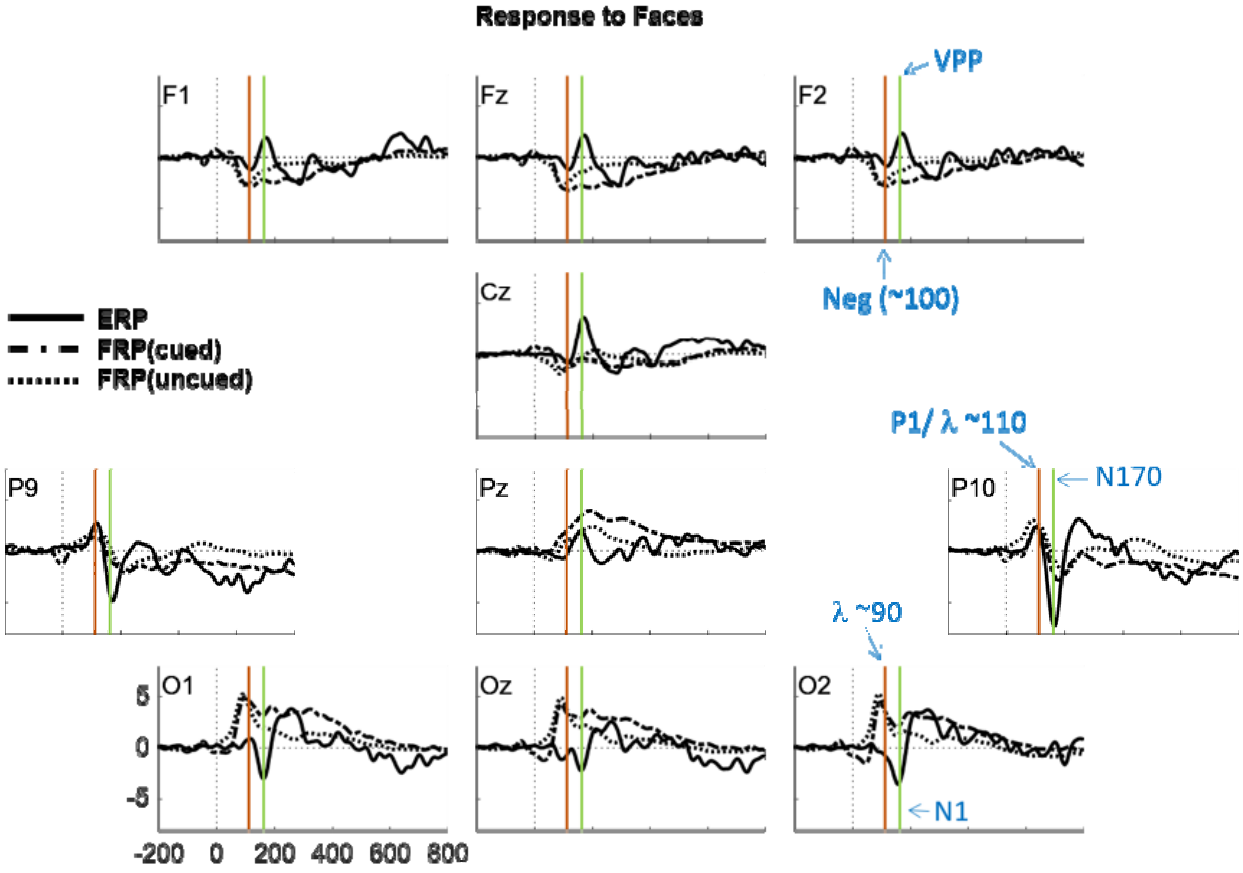
Response to Faces
F1
Fz
F2
VPP
Neg (~100)
Cz
ERP
FRP(cued)
FRP(uncued)
P1/ λ ~110
P9
Pz
P10
N170
λ ~90
O1
Oz
O2
N1
5
0
-5
-200
0
200
400
600
800

Figure 5

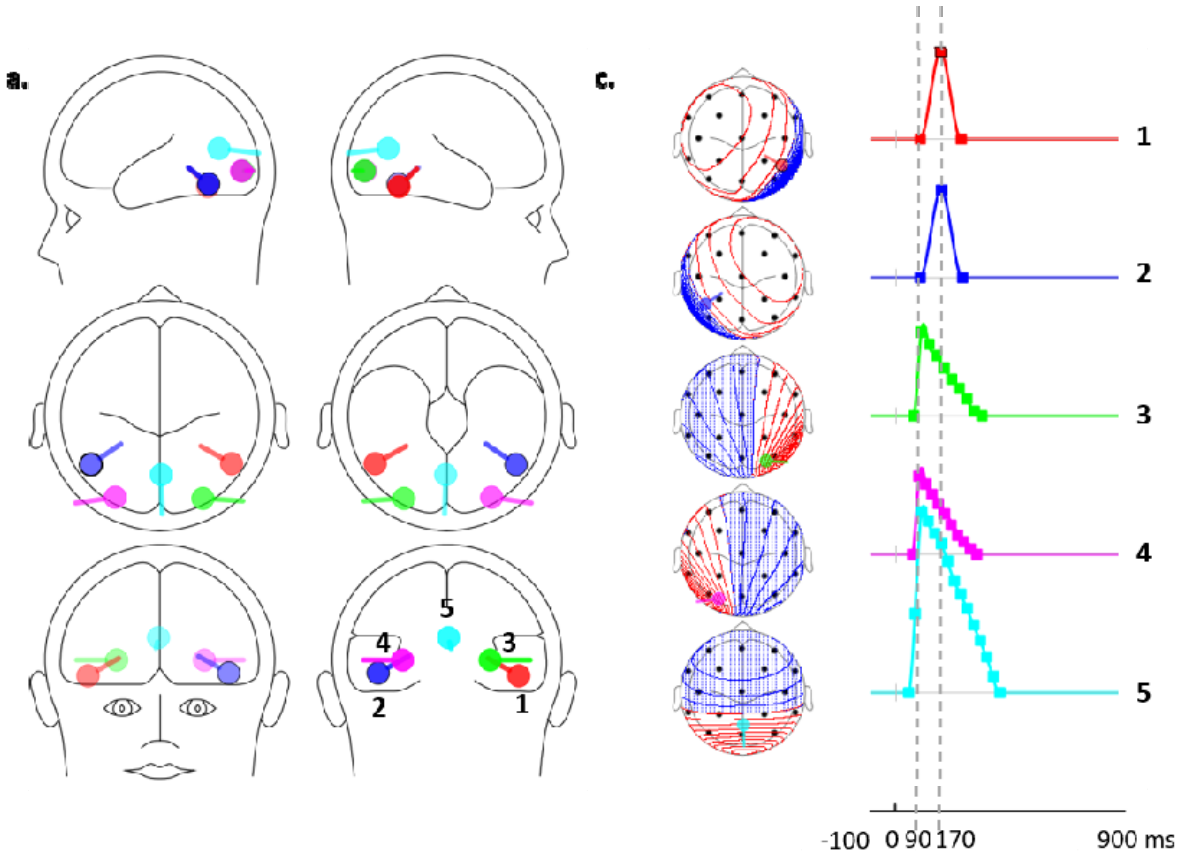

b.

	loc x	loc y	loc z	ori x	ori y	ori z	area
1 N1 right	50	- 57	-16	-0.779	0.389	0.492	R. Fusiform (37)
2 N1 left	-48	-58	-14	0.747	0.465	0.475	L. Fusiform (37)
3 P1 right	30	-89	-7	0.998	-0.063	-0.007	R. Visual Assoc. (18)
4 P1 left	-31	-88	-7	-0.99	-0.143	-0.012	L. Visual Assoc. (18)
5 Lambda	1	-70	12	0.025	-0.973	-0.231	Calcarine Fissure (17)

Figure 6

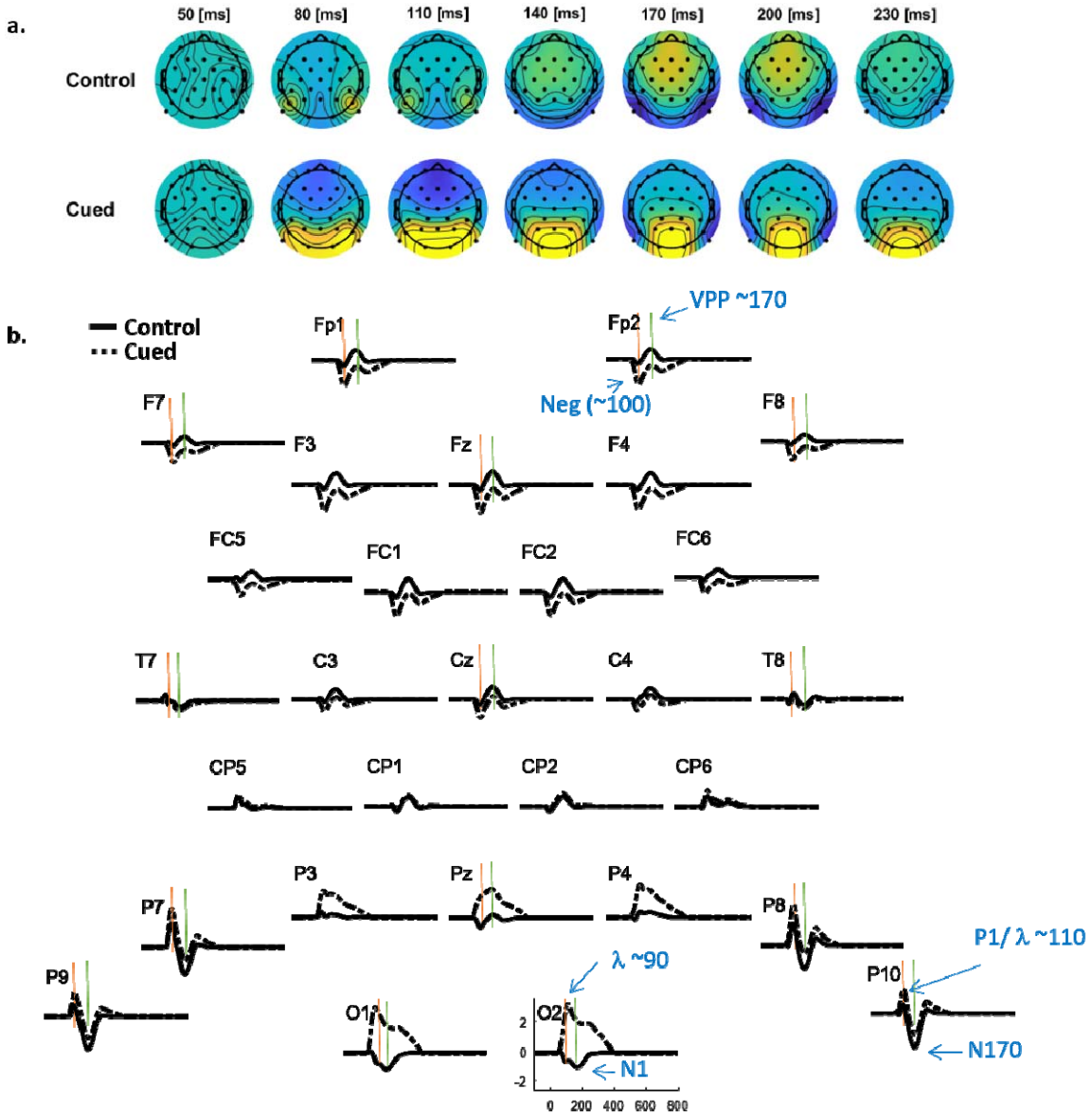
a.
50 [ms]
80 [ms]
110 [ms]
140 [ms]
170 [ms]
200 [ms]
230 [ms]
Control
Cued
b.
Control
Cued
VPP ~170
Neg (~100)
Fp1
Fp2
F7
F3
Fz
F4
F8
FC5
FC1
FC2
FC6
T7
C3
Cz
C4
T8
CP5
CP1
CP2
CP6
P7
P3
Pz
P4
P8
P9
P10
P1/ λ ~110
λ ~90
O1
O2
N1
N170
2
0
-2
0
200
400
600
800